International Journal on Magnetic Particle Imaging
Vol 8, No 1, Suppl 1, Article ID 2203020, 4 Pages

Infinite Science Publishing

Proceedings Article

Deep learning MPI super-resolution by implicit representation of the system matrix

Franziska Schrank [a,*] · Dennis Pantke [a] · Volkmar Schulz [a,b,c,d,*]

[a] Department of Physics of Molecular Imaging Systems, Institute for Experimental Molecular Imaging, RWTH Aachen University, Aachen, Germany
[b] Hyperion Hybrid Imaging Systems GmbH, Pauwelsstrasse 19, 52074 Aachen, Germany
[c] III. Physikalisches Institut B, Otto-Blumenthal-Strasse, 52074 Aachen, Germany
[d] Fraunhofer Institute for Digital Medicine MEVIS, Forckenbeckstrasse 55, Aachen, Germany
[*] Corresponding author, email: franziska.schrank@pmi.rwth-aachen.de, volkmar.schulz@pmi.rwth-aachen.de

Abstract

Image reconstruction in MPI is often performed with the system matrix (SM) approach, where the signal of a reference particle sample is measured on a predefined grid in the scanner. This calibration measurement is not only very time-consuming but also places an upper limit to the spatial resolution of the reconstructed image, given by the spacing between two adjacent SM grid points. Recently, implicit neural representations have shown great results in computer vision. They allow for oversampling to gain a higher frequency explicit representation of an object without fixing a certain upsampling scale. We show that this can be used to mostly restore an SM with up to 16x subsampling in 2D and to generate SMs of arbitrary size as an additional tool for image quality improvement. However, we also found that classic spline interpolation is a reasonable tool for this task as well.

I. Introduction

Currently, for the system matrix-based reconstruction approach, one needs to calibrate the system first. During this calibration, the scanner characteristics, acquisition scheme, and particle properties are encoded in the system matrix (SM) [1]. This is a time-consuming process as for example the calibration of a grid of $37 \times 37 \times 37$ voxels takes about 33 h, in which the system is inaccessible and it must be repeated whenever changes in the system or the used particles occur. Furthermore, the SM's gridding provides an upper limit for the spatial resolution of the image that is reconstructed using this SM, adding to image quality degradations due to system noise and background [2]. Reducing the calibration time in general as well as reducing the calibration time for smaller step-sizes in the SM are of high interest in MPI research.

In frequency domain, the SM components feature a spatial dependence, which can be visualized as oscillatory spatial patterns. Thus, techniques from computer vision are an obvious choice to perform tasks like denoising or resolution enhancement. In the last decades, deep learning has become a powerful tool in both computer vision and medical imaging for various tasks, including image super-resolution. For MPI, Baltruschat et al. [3] have shown that it is possible to recover a high-resolution SM from a lower resolution one using a neural network, which they trained with pairs of low- and high-resolution SM components. While this approach benefits from the supervised training manner, it is limited to a fixed upsampling scale by the network architecture, which implies that both input and output size are predefined. In this work, we focus on a super-resolution approach using a continuous representation of the SM by leveraging local implicit image functions.

I.I. Local implicit image function

The concept of implicit representations arose from the fact that the visual world is continuous and only machines require the description of objects by discrete samples. Modeling an object by a function that maps coordinates to their corresponding signal (RGB values in case of an image) enables to generate the object at arbitrary resolutions. This mapping function is parametrized by a neural network. Besides only using coordinates as inputs, Chen et al. propose the local implicit image function (LIIF) representation as an additional input, in form of local latent codes from the original image [4]. Their method consists of two networks, an encoder to extract the latent codes, which is trained in a self-supervised task together with a decoding network that takes the coordinates as inputs, queries the latent codes around these coordinates, and then predicts the RGB values.

We propose to use this approach to learn a generalizable continuous representation of the MPI SM to both restore undersampled matrices that can be acquired very quickly and to generate arbitrarily high resolved matrices for better image quality in reconstructed images.

II. Materials and methods

For training of the LIIF network, we use an SM from OpenMPIData [5], acquired with synomag®-D particles on a grid of $37 \times 37 \times 37$ voxels covering a volume of $(37 \times 37 \times 18.5)$ mm. Prior to training, SM frequency components are selected by applying an SNR threshold of 3 and only using frequencies above 80 kHz and below 600 kHz, to eliminate noisy components. The components are split 90/10 for training/validation and only the central slice (slice 19) of each 3D frequency component is used because it has high signal intensity, and it is RGB encoded following [6]. Training is performed using the original architecture of the LIIF network using the RDN encoder [7] and cell decoding. The network is pretrained on the DIV2K dataset [8], which contains natural high-resolution RGB images, unrelated to MPI. In the network fine-tuning, varying upsampling scales are included by sampling a random scale r from the uniform distribution $\mathcal{U}(1,4)$ for every image and cropping a patch of size $9r \times 9r$ from the image. The network input is given by downsampling the patches to 9×9 pixels and the ground-truths by sampling 9^2 pixel samples (coordinate-RGB pairs) from the patches so that the shape of all ground-truths in a batch is the same. The model is trained for 1000 epochs with a batch size of 256. All other parameters are the same as in the original paper [4].

Testing is performed on a second SM from OpenMPIData, which is acquired with the tracer perimag®. Measurements of the OpenMPIData resolution phantom are reconstructed using the Kaczmarz algorithm with Tikhonov regularization, where the regularization parameter is $\lambda = 0.01$, for 3 iterations. First, SM recovery is evaluated by downsampling the test SM by a factor 16 and using the trained LIIF network to recover the original resolution. Downsampling is performed by taking every fourth voxel along both width and height of the image. Second, the network is used on the test SM in original resolution to generate 16 times higher resolution. The LIIF network is compared to using classic spline interpolation with order 3. The SM recovery task was also performed using compressed sensing on a ratio of 1/16 random pixels from the original SM which was not feasible to recover most of the frequency components.

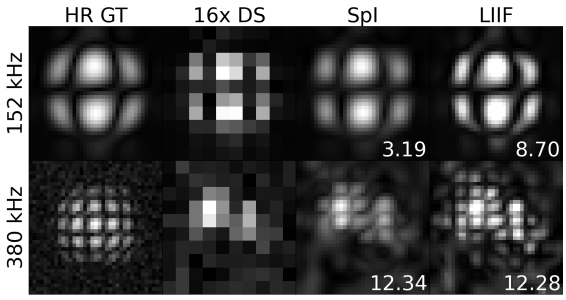

Figure 1: Two different frequency components of the high-resolution ground-truth SM (HR GT), the 16x downsampled SM (16x DS), the recovered SM using spline interpolation (SpI) and using the LIIF network (LIIF). NRMSE values are given in %.

III. Results and discussion

In Figure 1, absolute values of the central slice (slice 19) of two frequency components can be seen. The mean normalized root mean squared error (NRMSE) over all frequencies between ground-truth and recovered components is 12.77 % and 9.92 % for the LIIF network and spline interpolation, respectively, which indicates an improved performance of the spline interpolation over the LIIF network. Visually, the LIIF network generates sharper edges, though both spline interpolation and LIIF also introduce significant artifacts in the higher frequency component. These artifacts also translate into the reconstructed resolution phantom, as can be seen in Figure 2. However, both restored SMs enable the reconstruction of the middle arm of the phantom, where the LIIF network slightly outperforms the spline interpolation. This is also confirmed by the NRMSE values of 7.02 % for LIIF and 7.55 % for spline interpolation.
Next, the performance of the LIIF network to generate 16 times higher resolution is tested. As input the original SM is used. The output resolution of 148×148 pixels was not seen during training. The results in comparison to spline interpolation can be seen in Figure 3, also including reconstructions of the resolution phantom. For the lower frequency component, the generated images look very similar, while for the higher component some differences

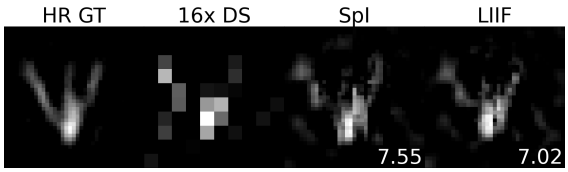

Figure 2: Reconstruction of the resolution phantom using the original high-resolution SM (HR GT), the 16x downsampled SM (16x DS) and the recovered SMs using spline interpolation (SpI) and the LIIF network (LIIF). NRMSE values are given in %.

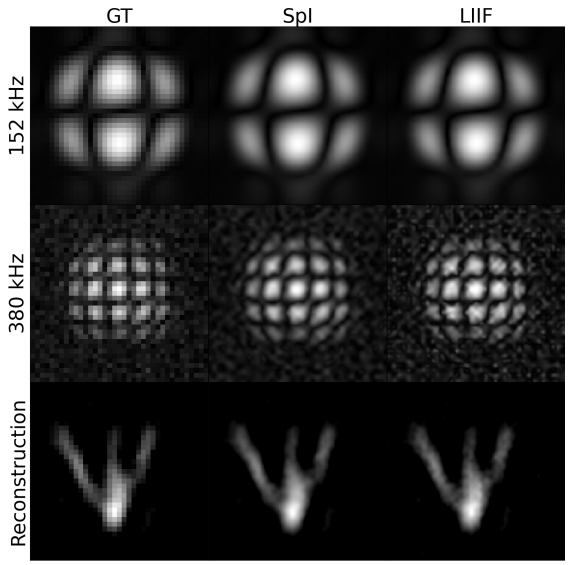

Figure 3: Two different frequency components of ground-truth SM (GT) and generated SMs using spline interpolation (SpI) and using the LIIF network (LIIF) and the corresponding reconstructions of the resolution phantom.

are visible. Both LIIF network and spline interpolation achieve an image that appears higher resolved, showing the distinct pattern of the component. Again, the edges in the pattern are slightly sharper for the LIIF network, while also being more distorted than using spline interpolation. The noise at the image borders also stands out less with the spline interpolation due to the overall higher degree of smoothness in the image. Reconstructions of the resolution phantom appear higher resolved in both cases, although no additional information is gained from the upscaling in comparison to the original reconstruction. The distortions from the LIIF network also translate into the phantom.

The performance of the LIIF network was expected to outperform spline interpolation by a larger margin but a reason for the opposite case could be the small size of the used SMs in general. Spline interpolation works well because the used SMs are very regular. For the future, it can be interesting to test less regular SMs, as well as to test the LIIF network on irregular grids. The latter could be useful to neglect single voxels from the SM measurement based on voxel-based SNR or to focus the network on a region of interest in the image center to prevent the augmentation of noise at the image borders. Including prior knowledge about the SM structure into the network training could also be an option.

IV. Conclusion

In this paper, we have shown that it is possible to mostly recover an SM with up to 16x subsampling in 2D with an approach based on local implicit image functions. For the used SMs, this amount of subsampling would result in a calibration time reduction of over 90 %. The proposed approach based on implicit representations can work with arbitrary resolutions and is not limited to the resolutions it has seen in training. However, for the used SMs, spline interpolation is another reasonable approach, which does not require any training. In an extension of this work, the LIIF network might be evaluated on irregular SM grids and modified to support the whole 3D volumes of the SM components. An approach to directly use the extracted latent codes for reconstruction should also be considered.

Acknowledgments

Research funding: We acknowledge the financial support by the German research foundation (DFG, grant number SCHU 2973/5-1).

Author's statement

Conflict of interest: Authors state no conflict of interest.

References

[1] J. Rahmer, J. Weizenecker, B. Gleich, and J. Borgert. Analysis of a 3-D System Function Measured for Magnetic Particle Imaging. *IEEE Transactions on Medical Imaging*, 31(6):1289–1299, 2012, doi:10.1109/TMI.2012.2188639.

[2] M. Straub and V. Schulz. Joint Reconstruction of Tracer Distribution and Background in Magnetic Particle Imaging. *IEEE Transactions on Medical Imaging*, 37(5):1192–1203, 2018, doi:10.1109/TMI.2017.2777878.

[3] I. M. Baltruschat, P. Szwargulski, F. Griese, M. Grosser, R. Werner, and T. Knopp. 3d-SMRnet: Achieving a new quality of MPI system matrix recovery by deep learning. *Medical Image Computing and Computer Assisted Intervention*, pp. 74–82, 2020, doi:10.1007/978-3-030-59713-9_8.

[4] Y. Chen, S. Liu, and X. Wang. Learning continuous image representation with local implicit image function. *IEEE/CVF Conference on Computer Vision and Pattern Recognition*, pp. 8628–8638, 2021.

[5] T. Knopp, P. Szwargulski, F. Griese, and M. Gräser. OpenMPIData: An initiative for freely accessible magnetic particle imaging data. *Data in Brief*, 28, 2020, doi:10.1016/j.dib.2019.104971.

[6] U. Heinen, A. Weber, J. Franke, H. Lehr, and O. Kosch. A versatile MPI System Function Viewer. *International Journal on Magnetic Particle Imaging*, 3(2), 2017, doi:10.18416/ijmpi.2017.1706006.

[7] Y. Zhang, Y. Tian, Y. Kong, B. Zhong, and Y. Fu. Residual dense network for image super-resolution. *IEEE Conference on Computer Vision and Pattern Recognition*, pp. 2472–2481, 2018.

[8] E. Agustsson and R. Timofte. NTIRE 2017 Challenge on Single Image Super-Resolution: Dataset and Study. *IEEE Conference on Computer Vision and Pattern Recognition Workshops (CVPRW)*, pp. 126–135, 2017, doi:10.1109/CVPRW.2017.150.